Proton NMR Studies of *Cucurbita maxima* Trypsin Inhibitors: Evidence for pH-Dependent Conformational Change and His25–Tyr27 Interaction†

Ramaswamy Krishnamoorthi,* Chan-Lan Sun Lin, and YuXi Gong‡
Department of Biochemistry, Kansas State University, Manhattan, Kansas 66506
David VanderVelde
Department of Medicinal Chemistry, University of Kansas, Lawrence, Kansas 66045
Karl Hahn
Health Sciences Center, University of Colorado, Denver, Colorado 80262
Received March 28, 1991; Revised Manuscript Received September 18, 1991

ABSTRACT: A pH-dependent His25–Tyr27 interaction was demonstrated in the case of *Cucurbita maxima* trypsin inhibitors (CMTI-I and CMTI-III) by means of nuclear magnetic resonance (NMR) spectroscopy. pH titration, line widths, peak shapes, deuterium exchange kinetics, and two-dimensional nuclear Overhauser effect spectroscopy (NOESY) were employed to characterize a conformational change involving Tyr27, which was shown to be triggered by deprotonation of His25 around pH 6. A hydrogen bond is proposed to be formed between N_ϵ of His25 and OH of Tyr27, as a distance between the atoms, His25 Nϵ and Tyr27 OH, of 3.02 Å is consistent with a model built with NOE-derived distance constraints. Both the X-ray [Bode, W., Greyling, J. H., Huber, R., Otlewski, J., & Wilusz, T. (1989) *FEBS Lett. 242*, 282–292] and NMR [Holak, T. A., Gondol, D., Otlewski, J., & Wilusz, T. (1989) *J. Mol. Biol. 210*, 635–648] structures of CMTI-I at low pH (4.7–5.3) rule out such an interaction between the two aromatic rings, as the ring planes are oriented about 10 Å away from each other. The presently characterized relative orientations of His25 and Tyr27 are of functional significance, as these residues make contact with the enzyme in the enzyme–inhibitor complex. Furthermore, trypsin assay and inhibitor-binding studies showed that conformations of trypsin and the squash inhibitor were functionally relevant only in the pH range 6–8. The pK_a of His25 was determined and found to be influenced by Glu9/Lys substitution and by the hydrolysis of the reactive-site peptide bond between Arg5 and Ile6. As these sites are located far (>10 Å) from His25, the results point out conformational changes that are propagated to a distant site in the protein molecule.

Serine proteinase inhibitors from the squash family comprise small proteins (3 kDa), each containing 29–32 amino acid residues, including three disulfide linkages (Wieczorek et al., 1985; Otlewski., 1990). Pumpkin seeds (*Cucurbita maxima*) contain three such inhibitor proteins, *Cucurbita maxima* trypsin inhibitor-I, -III, and -IV (CMTI-I, CMTI-III, and CMTI-IV).[1] CMTI-III differs from CMTI-I by a single residue substitution: Lys9 in place of Glu (Wieczorek et al., 1985). Both the solid (Bode et al., 1989) and solution structures (Holak et al., 1989a,b) of CMTI-I have been determined, and they are found to be the same. The reactive site has been shown to be the peptide bond between Arg5 and Ile6 (Wieczorek et al., 1985). CMTI's inhibit biologically important molecules such as activated Hageman factor, otherwise known as factor XII_a, a blood coagulation factor (Hojima et al., 1982), human leukocyte elastase, and cathepsin G (McWherter et al., 1989).

One approach to developing designs for inhibitors of modified functions and/or efficacy would be to evaluate structural consequences of naturally occurring substitutions as found in CMTI-I and CMTI-III. In the preceding paper (Krishnamoorthi et al., 1992), we demonstrate, by two-dimensional nuclear magnetic resonance (2D NMR) spectroscopy, that both the reactive-site peptide bond cleavage and the substitution of Glu9 by Lys lead to perturbations causing tertiary structural changes for residues located near and far from the reactive site/substitution site, in particular, those located in the C-terminal half of the molecule. However, the secondary structural elements are not affected. In this paper, we provide experimental evidence for the conformational consequences of reactive-site peptide bond hydrolysis and Glu9/Lys substitution by determining the pK_a of His25 in CMTI-I and CMTI-III and their modified forms, CMTI-I* and CMTI-III*. His25 is located in the C-terminal part of the CMTI molecule, at least 10 Å away from the Arg5–Ile6 peptide bond, and a similar distance from $C_\alpha H$ of the ninth amino acid residue. During the course of that investigation, we have discovered, on the basis of peak shapes, line widths, deuterium exchange kinetics, and nuclear Overhauser effect (NOE) data, an interaction between His25 and Tyr27 that is triggered by the ionization of the histidine residue. Distance constraints obtained from NOE measurements established that a conformational chagne involving a rotation about the α–β bond of Tyr-27 occurs, and a hydrogen bond is formed between OH of Tyr27 and N_ϵ of His25. This interaction vanishes at low pH, where histidine is protonated, or at high pH (above 11), where tyrosine is predominately dissociated. The neutral pH

† This study was supported by grants from the American Heart Association, Kansas Affiliate, and the Wesley Foundation, Wichita, KS (to R.K.).
* To whom correspondence should be addressed.
‡ Permanent address: Testing Center, Hubei Academy of Agricultural Science, Wuhan, China.

[1] Abbreviations: CMTI, *Cucurbita maxima* trypsin inhibitor; 2D NMR, two-dimensional nuclear magnetic resonance; ppm, parts per million, DQF-COSY, double-quantum filtered correlated spectroscopy; TOCSY, total correlated spectroscopy; NOE, nuclear Overhauser effect; NOESY, 2D NOE spectroscopy; BAPNA, benzoyl-L-Arg-*p*-nitroanilide.

0006-2960/92/0431-905$03.00/0

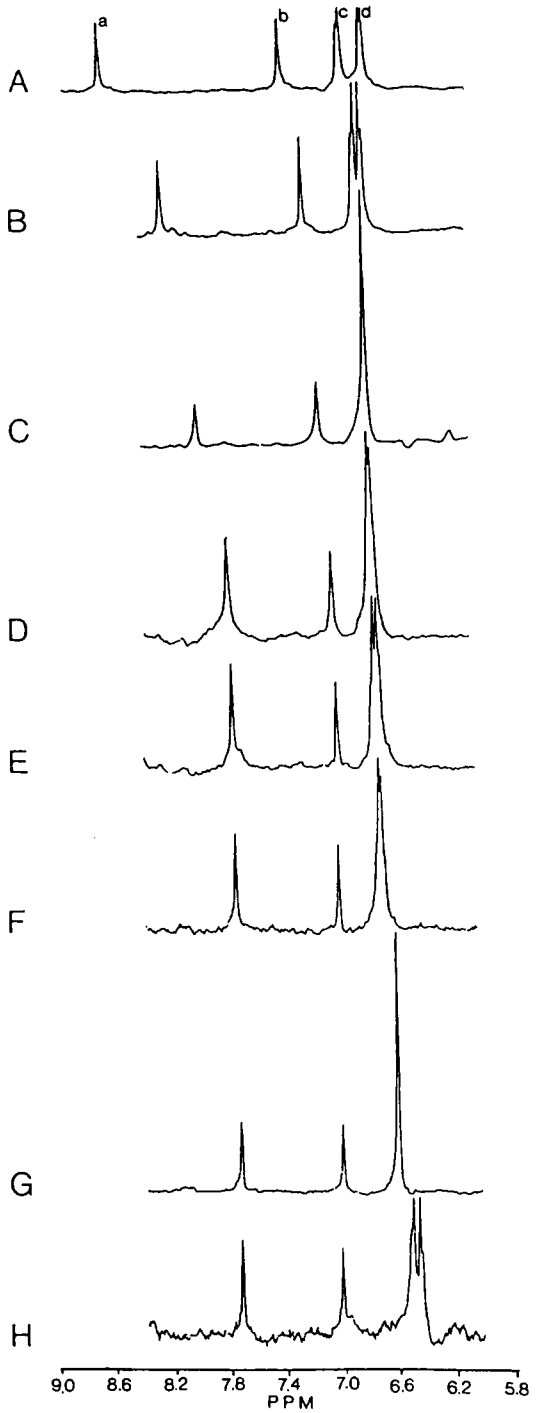

FIGURE 1: Aromatic region of 400-MHz ^1H NMR spectra of *Cucurbita maxima* trypsin inhibitor I (CMTI-I) in ^2H_2O at 30 °C at selected pH's: (A) 4.05; (B) 5.75; (C) 6.25; (D) 7.50; (E) 9.00; (F) 10.02; (G) 11.01; (H) 12.16. Peaks a and b are assigned to $C_\epsilon H$ and $C_\delta H$ of His25, respectively, and peaks c and d are assigned to H_δ's and H_ϵ's of Tyr27, respectively.

conformation is thus in contrast to both the X-ray (Bode et al., 1989) and NMR (Holak et al., 1989a,b) structures of CMTI-I at low pH (below 5), which indicate the absence of a His25–Tyr27 interaction, as the two aromatic ring planes are oriented about 10 Å away from each other. The neutral pH form of CMTI is relevant, because trypsin is active only above pH 6. The pK_a of His25 is affected both by the Glu9/Lys substitution (between CMTI-I/CMTI-III) and the reactive-site peptide bond (Arg5–Ile6) hydrolysis.

Materials and Methods

Proteins. CMTI-I and CMTI-III and their reactive-site modified forms, CMTI-I* and CMTI-III* were isolated and purified from pumpkin seeds by means of trypsin-affinity chromatography and reverse-phase high-performance liquid chromatography (HPLC), as described by Krishnamoorthi et al. (1990). A typical NMR sample was prepared by dissolving a weighed amount of lyophilized protein (5–9 mg) in 0.4 mL of ^2H_2O, and adjusting the pH to the desired value with 0.2 M NaO^2H or 0.2 M ^2HCl, followed by centrifugation. The pH measurements were carried out with a Fisher pH meter (model 815 MP), using an Ingold microcombination glass electrode. The reported pH values are meter readings, uncorrected for the isotope effect. Samples for measuring deuterium exchange kinetics of $C_\epsilon H$ and $C_\delta H$ of the single histidine residue (His25) were prepared by dissolving lyophilized protein whose solvent-labile hydrogens had been preexchanged with deuterons. The deuterium exchange of the $C_\epsilon H$ and $C_\delta H$ was followed by measuring peak heights periodically at 30 °C. The sample was maintained in a constant temperature bath for this study. The amount of time taken to collect spectra was negligible in comparison to the rate of decrease of peak intensity. Trypsin and substrate, benzoyl-L-Arg-*p*-nitroanilide (BAPNA), were purchased from Sigma. All other chemicals used were of reagent grade or better.

NMR Spectroscopy. One-dimensional ^1H NMR spectra of the inhibitor proteins were collected using a Bruker 400-WM spectrometer (400 MHz for ^1H). The residual solvent peak was saturated by a decoupler-pulse off acquisition. Chemical shifts were referenced by assigning a value of 4.71 ppm to the water peak at 30 °C. Line widths were measured by using the Lorenzian line-fit program available from the Bruker software. The two-dimensional total correlated spectroscopy (TOCSY) experiment was performed at 500 MHz with a Bruker 500 AM instrument, using an MLEV17 spin lock (Braunschweiler & Ernst, 1983; Bax & Davis, 1985) with a mixing time of 70 ms. The two-dimensional NOE experiment (NOESY) was performed according to the standard NOESY pulse sequence (Anil Kumar et al., 1980) using a mixing time of 200 ms. Data were collected using the time-proportional phase incrementation (TPPI) method (Marion & Wüthrich, 1983). A total of 2048 data points were used in the F_2 dimension and 512 in the F_1 dimension, which

Table I: NOE-Derived Distance Constraints between Tyr27 H_δ's and Various Assigned Hydrogens of CMTI-III* at pH 7.92[a]

atom	distance (Å)[b]	atom	distance (Å)[b]
Lys9 H_α	3.5 (2.37)	His25 $H_{\beta 2}$	4.6 (4.51)
Tyr27 H_α	3.6 (2.42)	Leu7, H_β	3.8 (7.46, 9.02)
His25 $H_{\beta 1}$	4.6 (4.76)	His25 $C_\epsilon H$	3.8 (8.12)

[a] The distance between H_δ and H_β's of Tyr27 was taken to be 3.2 Å. [b] Numbers within parentheses are the corresponding distances in angstroms for low pH (4.7–5.3) form of CMTI-I, as determined by Holak et al. (1989a).

Table II: Chemical Shift Changes of Residues in CMTI-III* That Are Influenced by pH-Dependent Conformational Change

residue	chemical shift (ppm)[a] pH 4.71	pH 7.92	difference[b] (ppm)
Arg1 $C_\alpha H$	4.12	4.22	0.10
Arg1 $C_\beta H$	1.92	1.86	−0.06
Ile6 $C_\alpha H$	3.87	3.67	−0.20
Ile6 $C_\beta H$	1.97	1.88	−0.09
Glu24 $C_\alpha H$	3.95	4.00	0.05
Glu24 $C_\beta H$	1.88, 1.98	2.07, 2.22	0.19, 0.24
His25 $C_\alpha H$	4.61	4.75	0.14
His25 $C_\beta H$	3.35, 3.58	3.13, 3.32	−0.22, −0.26
Gly26 $C_\alpha H$	3.78, 4.00	3.67, 4.02	−0.11, 0.02
Tyr27 $C_\alpha H$	5.45	5.32	−0.13
Tyr27 $C_\beta H$	2.73	2.42	−0.31

[a] Accuracy ±0.02 ppm. [b] (Chemical shift at pH 7.92) − (chemical shift at pH 4.71).

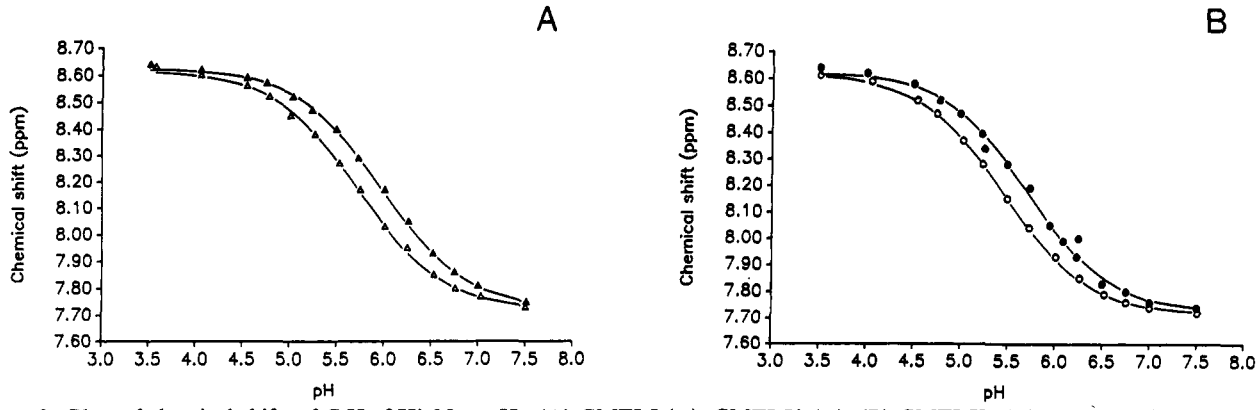

FIGURE 2: Plots of chemical shifts of $C_\epsilon H$ of His25 vs pH. (A) CMTI-I (△); CMTI-I* (▲); (B) CMTI-III (○); CMTI-III* (●). CMTI-I has a Glu in position 9, whereas CMTI-III has a Lys residue (Wieczorek et al., 1985).

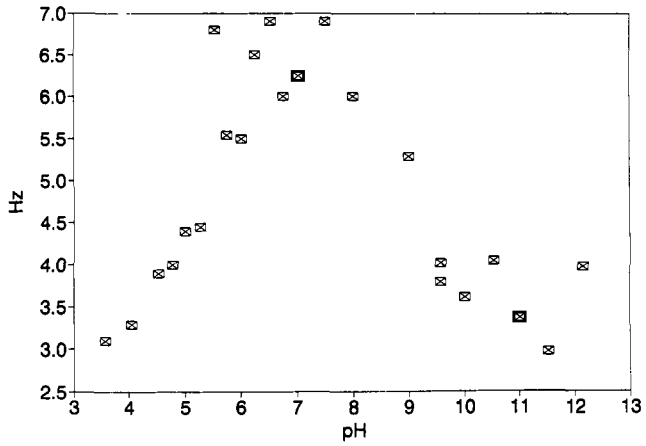

FIGURE 3: Plot of line width of $C_\epsilon H$ of His25 of CMTI-I vs pH. The plot indicates the presence of an exchange process in the pH range 7–12.

was zero-filled once before processing. NOESY cross-peak intensities were estimated from the appropriate 2D slice.

Trypsin Activity Assays. Trypsin activity (32 μM) was assayed by following the rate of hydrolysis of the substrate, BAPNA (0.69 M), in the presence and absence of CMTI-III*, spectrophotometrically at 405 nm at various pH's. Less than the stoichiometric amount of the inhibitor was used at each pH to determine the effect of pH on the binding of the inhibitor to the enzyme. The molar extinction coefficient of the resulting *p*-nitroaniline is independent of pH in the range 5–10.5 (Erlanger et al., 1961).

Molecular Modeling. The NMR coordinates for CMTI-I (Holak et al., 1989a) were loaded into Sybyl (Tripos Associates, St. Louis, MO) using the Brookhaven format, and disulfide bonds were generated between Cys16–Cys28, Cys10–Cys22, and Cys3–Cys20. Glu9 was changed to Lys9 after which all protein dictionary hydrogens were added. Relative distances from Tyr-27 $H_{\delta 1}$ and nearby assigned hydrogens were estimated by measuring cross-peak intensities from the appropriate NOESY slice, assigning a value of 3.2 Å to the distance between $H_{\delta 1}$ and $H_{\beta 1}/H_{\beta 2}$, using the equation (Borgias & James, 1989)

$$\sigma_1/\sigma_2 = (r_2/r_1)^6$$

where σ's are the cross-peak intensities and r's are the relative distances between assigned hydrogen atoms and Tyr27 $H_{\delta 1}$ (Borgias & James, 1989). These values were incorporated into the molecular description as simple distance constraints. Due

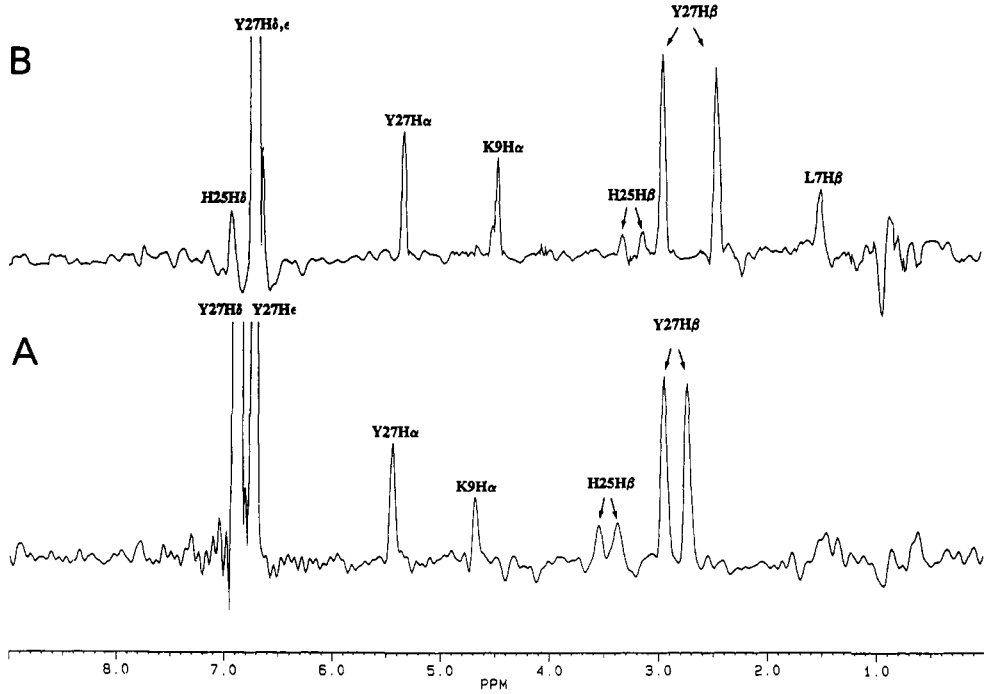

FIGURE 4: NOESY cross section taken parallel to F_1 dimension at the chemical shift position corresponding to that of Tyr27 H_δ's at two different pH's. (A) 4.71; (B) 7.92. The low pH form assignments (Krishnamoorthi et al., 1992) have been obtained by sequential assignment procedures (Wüthrich et al., 1982). The neutral pH form assignments were obtained by correlation (see text).

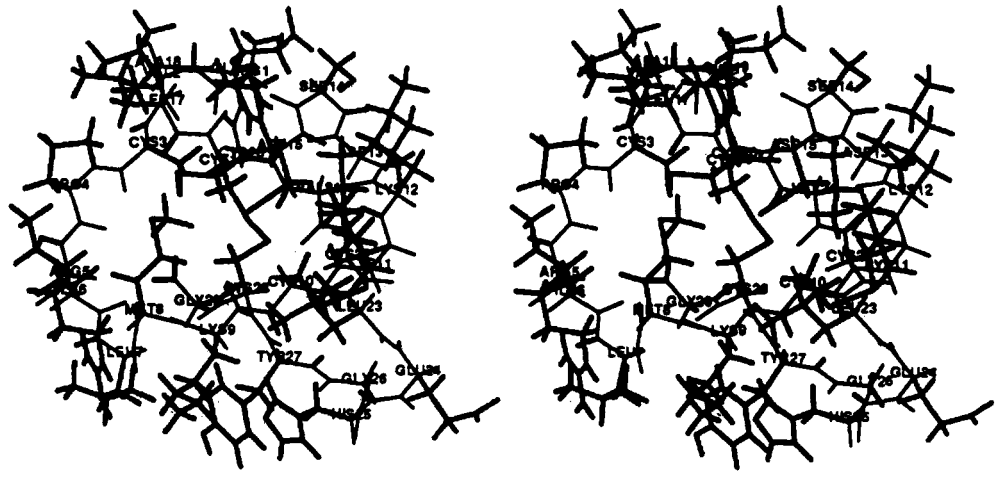

FIGURE 5: Stereodiagrams of relative orientations of His25 and Tyr27 in CMTI-III* generated by using the NOE-derived distance constraints at neutral pH (7.92) in conjunction with the NMR coordinates of CMTI-I (Holak et al., 1989a) at low pH (4.7–5.3). In the low pH form the two aromatic rings are oriented 10 Å away from each other, and no interaction exists; in contrast, for the neutral pH form, a hydrogen bond is indicated between N_ϵ of His25 and OH of Tyr27, as the distance between the atoms of N and H is computed to be 3.02 Å.

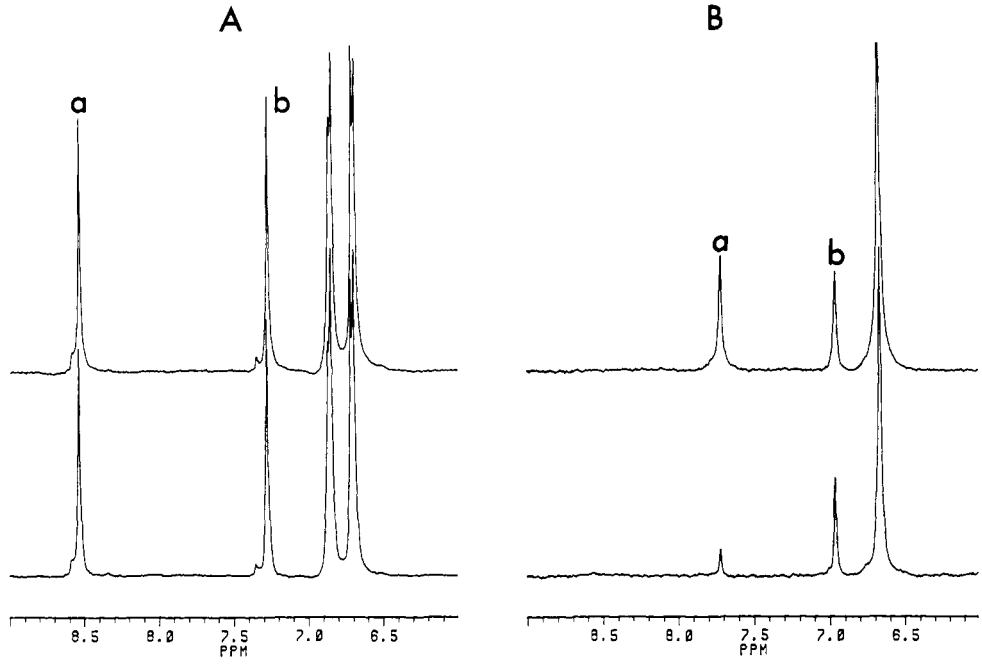

FIGURE 6: Deuterium exchange of $C_\delta H$ and $C_\epsilon H$ of His25 of CMTI-III* at two pH's: (Panel A) 4.71. The top trace corresponds to $t = 0$, and the bottom trace corresponds to $t = 21$ days; (Panel B) 7.92. The top trace corresponds to $t = 0$, and the bottom trace corresponds to $t = 47$ days. Peaks a and b are assigned to the $C_\epsilon H$ and $C_\delta H$, respectively, of His25. The $C_\delta H$ did not undergo any detectable exchange over a period of 47 days at pH 7.92. There are residual slowly exchanging amide hydrogens underneath Tyr27 signal at pH 7.92, causing an anomaly in its intensity with time.

to the large distance between the His and Tyr rings in the starting structure, difficulties in generating appropriate starting conformations for molecular mechanics were encountered. On the basis of initial interactive bond rotation and initial minimizer runs, it was found that positioning the side chain of Tyr27 by changing χ^1 to 40° and χ^2 to 90° moved the rings close enough to begin mechanics. Using this starting structure, the Sybyl 5.3 conjugate gradient minimizer without electrostatics was run using default energy change convergence parameters. The force field (TRIPOS 5.2) was modified slightly to optimize aromatic ring planarity (Clark et al., 1989; Clark, 1990). Simplex techniques were used as required to repair initial bad geometry. The molecular model displayed in relaxed stereo (Figure 5 and Table I) satisfies distance constraints to within about 1%, but the hydrogen-bond geometry, while meeting the distance constraint of 3 Å between Tyr27 OH and His25 N_{ϵ_2}, is distorted. Other models, generated from different starting configurations and using angle constraints, resulted in a less distorted hydrogen-bond geometry at the expense of considerably larger deviations from assigned NOE-based distances.

Results and Discussion

Figure 1 displays the aromatic region of the 400-MHz NMR spectra of virgin CMTI-I dissolved in ^2H_2O at 30 °C at selected pH values. As the pH is raised gradually from 4.05 (trace A), the $C_\epsilon H$ and $C_\delta H$ peaks of His25 (peaks a and b, respectively) shift upfield, as expected. However, more interesting and unique are the changes exhibited by Tyr27 ring hydrogens (peaks c and d): At low pH, the aromatic ring peaks exhibit the expected AA′XX′ spin pattern, but as the pH is raised, the peaks coalesce. For example, at pH 6.25 (trace C), we see only one peak for the four ring hydrogens of Tyr27. As the pH is raised, the peaks undergo further changes: they separate and coalesce again at pH 11, and, at pH 12.16, where tyrosine is expected to have ionized, the peaks regain the normal AA′XX′ pattern. Similar spectral changes were observed for the reactive-site modified CMTI-I

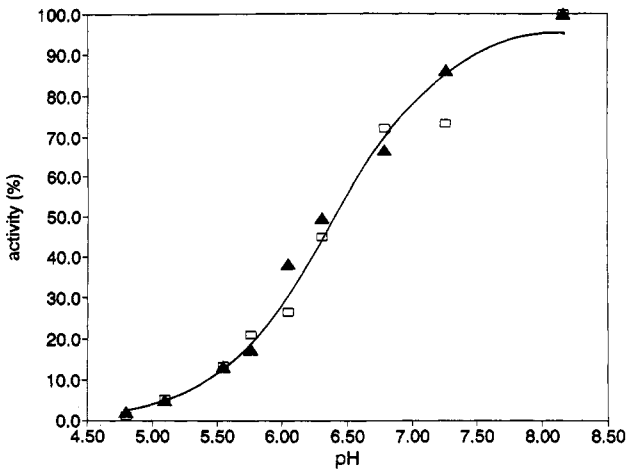

FIGURE 7: Trypsin activity as a function of pH: (▲) data points for free enzyme alone; (□) data points for the residual enzyme after less than 1 equiv of the inhibitor CMTI-III* has been added. Trypsin activity is modulated by an ionizing group with a pK_a of 6.36 ± 0.06.

(CMTI-I*), virgin CMTI-III, and reactive-site hydrolyzed CMTI-III (CMTI-III*). From plots of chemical shifts vs pH for the histidine $C_\epsilon H$ (peak a; Figure 2A,B), the following pK_a values (±0.02) were obtained for His25 in virgin and modified forms of the two inhibitors: 5.72 (CMTI-I); 5.97 (CMTI-I*); 5.47 (CMTI-III); 5.71 (CMTI-III*). A simple proton-dissociation equilibrium equation was used for the fit. CMTI-I and CMTI-III differ from each other by the substitution of Glu9 in CMTI-I by Lys in CMTI-III. The modified inhibitors each have the Arg5–Ile6 peptide bond hydrolyzed. An examination of the NMR coordinates obtained for CMTI-I in the pH range 4.7–5.1 indicates that atoms of residues Arg5 and Ile6 are within a distance of 12.7–17.6 Å from $N_\delta H$ of His25,; atoms of Glu9 are within a distance of 9.5–12.7 Å from $N_\delta H$ of His25, and they are not involved directly in any interaction with atoms of His25 (Bode et al., 1989). Therefore, it is concluded that the Glu9/Lys substitution, as well as Arg5–Ile6 hydrolysis, results in conformational changes of the inhibitor that are transmitted over a considerable distance as indicated by the pK_a values of His25.

Figure 3 depicts a plot of line width of His25 $C_\epsilon H$ of CMTI-I as a function of pH. Normally, one would expect the line width to increase and reach a maximum at or near the pK_a (±0.3 unit), depending upon acid/base catalysis of the ionization equilibrium, and then return to its normal value in the base form, i.e., at a pH equal to pK_a + 1.5 (Sudmeier et al., 1980). However, Figure 3 shows an anomalous behavior: The line widths reaches a maximum of about 7 Hz around pH 7, and it slowly returns to the expected limit of about 3 Hz near pH 12, where tyrosine is expected to have ionized. In other words, the line width of His25 $C_\epsilon H$ has an excess contribution, even after its pK_a (5.72) has been exceeded by more than 3 units. The possibility of protein aggregation is ruled out because the line width of a resolved methyl peak does not change over the entire pH range studied. The excess line width, therefore, indicates the presence beyond pH 7 of a chemical exchange process in which the deprotonated aromatic ring of His25 participates. Similar line width plots were obtained for CMTI-I*, CMTI-III, and CMTI-III*. In each case a maximum line width of about 8–10 Hz was observed. The increase in line width at pK_a represents an exchange contribution due to the dynamic equilibrium between the protonated and deprotonated form of His25, and it appears that all four forms of the inhibitor have the same dynamic properties, although the pK_a of His25 varies from one protein to another. The average lifetime of the His25 ring in one conformational state (τ) was estimated from line-broadening ($\delta\nu$) to be about 40 ms by means of

$$\tau = 1/\pi(\delta\nu)$$

Figure 4 compares the cross section taken from a NOESY map at the chemical shift position corresponding to that of Tyr27 $H_{\delta 1}$ at low pH (Figure 4A) and at neutral pH, i.e., 7.92 (Figure 4B). The data were obtained for CMTI-III*. Sequence-specific proton assignments for CMTI-III* at low pH (4.71) have been obtained (Krishnamoorthi et al., 1992) by following the standard 2D NMR procedures (Wüthrich et al., 1982; Wüthrich, 1986). Cross peaks from the neutral pH form were correlated to those of the low pH form by means of TOCSY experiments (not shown). Peaks from α-hydrogens of Ile6, Gly26, and Tyr27, and from β-hydrogens of Arg1, Ile6, His25, and Tyr27 move upfield, whereas peaks from α-hydrogens of Arg1, Glu24, and His25, and β-hydrogens of Glu24 move downfield (Table II). The key result is the observation of two NOE cross peaks at 6.9 and 1.5 ppm (Figure 4B); these cross peaks are not observed at low pH. The full NOESY contour map of CMTI-III* at low pH (not shown) does not show any cross peaks between His25 and Tyr27 ring hydrogens. The 6.9 ppm cross peak shown in Figure 4B is easily assigned to the NOE between $C_\delta H$ of His25 and $H_{\delta 1}$ of Tyr27. From the full NOESY map (not shown), it was found that the 1.5 ppm cross peak could be assigned either to the methyl of Ala18 or $C_\beta H$'s of Leu7. The Ala18 methyl group is located about 16 Å from His25, whereas Leu7 $C_\beta H$'s are located about 7.5–9.0 Å distant (Bode et al., 1989). Because Leu7 is located closer to His25 at low pH, we assign the 1.5 ppm cross peak to $C_\beta H$ of Leu7. Obviously, conformational changes above pH 6 have brought these hydrogens to within 4 Å since an NOE cross peak is observed. Because the H_δ and H_ϵ peaks of Tyr27 overlap at this pH, there is uncertainty in assigning the origin of some of the NOE cross peaks. All three residues, viz., Leu7, His25, and Tyr27, make contacts with atoms of trypsin in the enzyme–inhibitor complex and hence are functionally relevant (Bode et al., 1989). The chemical shift of one of the $C_\beta H$'s of Tyr27 changes by –0.31 ppm and those of $C_\beta H$'s of His25 change by –0.22 and –0.26 ppm as a result of the His25–Tyr27 interaction. These chemical shift changes arise most likely out of a contribution from the ring currents of His25 and Tyr27. Distances between $H_{\delta 1}$ of Tyr27 and assigned hydrogens were estimated from cross-peak intensities (Table I) and used to obtain the relative orientations of Tyr27 and His25 residues (Figure 5). A hydrogen bond is proposed to be formed between the OH of Tyr27 and N_ϵ of His25. This distance is estimated to be about 3 Å from the proposed neutral pH model; the corresponding distance for the low pH form is 10.16 Å (Holak et al., 1989a). This new conformation appears to differ from the earlier structures mainly by the rotation around the α–β bond of Tyr27. The (His25)N_ϵ···HO(Tyr27) hydrogen bond is abolished when the pH is raised beyond 11, where the ionized form of Tyr is expected to be dominant. Similarly, when His25 is protonated below its pK_a, the interaction is removed. A temperature dependence study of CMTI-III* at pH 7.51 indicated that at 60 °C, the coalesced peak of Tyr27 began to show its AA'XX' spin pattern, thus indicating the thermal breaking of the hydrogen bond (spectra not shown).

One consequence of the His25–Tyr27 interaction is the reduced accessibility of His25 $C_\delta H$ to solvent for deuterium exchange: Deuterium exchange measurements indicated that at low pH (4.71) the $C_\epsilon H$ and $C_\delta H$ of His25 (peaks a and b; Figure 6A) exchanged with the isotope with half-lives of 153 and 227 days, respectively. At neutral pH (7.92), while $C_\epsilon H$ exchanged with a half-life of 23.3 days, i.e., about 6.6 times faster, the $C_\delta H$ did not show any detectable change in intensity

over a period of 47 days (Figure 6B). If there were no differential effects on the rate of exchange of $C_\delta H$ of His25, then it would have undergone deuterium exchange with a half-life of 34.6 days. In fact, the stereopicture of CMTI-III at pH 7.92 (Figure 5) indicates a solvent-inaccessible position for the $C_\delta H$ of His25.

The presently determined relative orientations of His25 and Tyr27 are of relevance, because trypsin is active only above pH 6 (Figure 7). The activity of trypsin is modulated by an ionizing group with a pK_a of 6.36 ± 0.06. The normalized activity measurements, which are expressed as percent of maximal activity observed for the residual enzyme after the addition of less than one equivalent amount of the inhibitor, essentially fall on the curve for the free enzyme, and thus indicate that the modified inhibitor binding is not affected by pH. However, the presently described relative orientation of His25 and Tyr27 is relevant in the pH range where both the enzyme and the inhibitor are functional, as both of these residues make contacts with the enzyme in the enzyme–inhibitor complex. Design of drugs or inhibitors of more potent activity may benefit by taking into account the presently characterized structural information.

Acknowledgments

R.K. thanks Drs. W. Bode and T. Holak for providing the X-ray and NMR coordinates of CMTI-I, respectively, and Professors J. L. Markley and G. R. Reeck for encouragement. This is publication 91-401-J of the Kansas Agricultural Experiment Station.

Registry No. CMTI-I, 84795-93-7; CMTI-III, 79044-57-8; His, 71-00-1; Tyr, 60-18-4; trypsin, 9002-07-7.

References

Anil Kumar, Ernst, R. R., & Wüthrich, K. (1980) *Biochem. Biophys. Res. Commun. 95*, 1–6.

Bax, A., & Davis, D. G. (1985) *J. Magn. Reson. 65*, 355–360.

Bode, W., Greyling, H. J., Huber, R., Otlewski, J., & Wilusz, T. (1989) *FEBS Lett. 242*, 285–292.

Borgias, B. A., & James, T. L. (1989) *Methods Enzymol. 176*, 169–183.

Braunschweiler, L., & Ernst, R. R. (1983) *J. Magn. Reson. 53*, 521.

Clark, M. (1990) *Sybyl Update: A Technical Newsletter 3*, 11–12.

Clark, M., Cramer, R. D., III, & Van Opdendosch, N. (1989) *J. Comput. Chem. 10*, 982–1012.

Erlanger, B. F., Kokowsky, N., & Cohen, W. (1961) *Arch. Biochem. Biophys. 95*, 271–278.

Hojima, Y., Pierce, J. V., & Pisano, J. J. (1982) *Biochemistry 21*, 3741–3746.

Holak, T. A., Bode, W., Huber, R., Otlewski, J., & Wilusz, T. (1989a) *J. Mol. Biol. 210*, 649–654.

Holak, T. A., Gondol, D., Otlewski, J., & Wilusz, T. (1989b) *J. Mol. Biol. 210*, 635–648.

Krishnamoorthi, R., Gong, Y., & Richardson, M. (1990) *FEBS Lett. 273*, 163–167.

Krishnamoorthi, R., Gong, Y. & Lin, C. S., & VanderVelde, D. (1992) *Biochemistry* (preceding paper in this issue).

Kupryszewski, G., Ragnarsson, U., Rolka, K., & Wilusz, T. (1986) *Int. J. Pept. Protein Res. 27*, 245–250.

Marion, D., & Wüthrich, K. (1983) *Biochem. Biophys. Res. Commun. 113*, 967–974.

McWherter, C. A., Walkenhorst, W. F., Campbell, E. J., & Glover, G. I. (1989) *Biochemistry 28*, 5708–5714.

Otlewski, J. (1990) *Biol. Chem. Hoppe-Seyler 371 Suppl.*, 23–28.

Sudmeier, J. L., Evelhoch, J. L., & Jonsson, B.-H. (1980) *J. Magn. Reson. 40*, 377–390.

Wieczorek, M., Otlewski, J., Cook, J., Parks, K., Leluk, J., Wilimowska-pelc, A., Polanowski, A., Wilusz, T., & Laskowski, M., Jr. (1985) *Biochem. Biophys. Res. Commun. 126*, 646–652.

Wüthrich, K. (1986) *NMR of Proteins and Nucleic Acids*, pp 1–292, Wiley, New York.

Wüthrich, K., Wider, G., Wagner, G., & Braun, W. (1982) *J. Mol. Biol. 155*, 311–319.

0006-2960/92/0431-910$03.00/0